

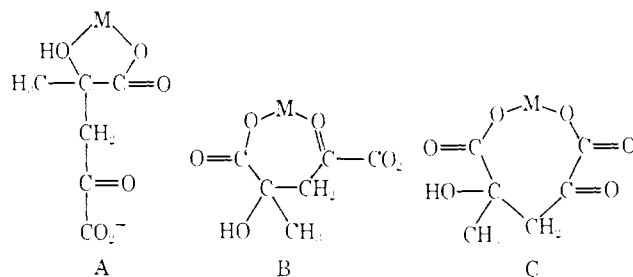
The values of pK_a for the two carboxylate groups of pyruvate dimer in Table I are comparable to values reported for acids which are similar to the dimer in structure. The α -keto end of the dimer structurally resembles the corresponding end of α -ketoglutaric acid ($pK_{1a} = 1.9, pK_{2a} = 4.56$)¹³ whereas the opposite end of the dimer is related to lactic acid ($pK_a = 3.74$),¹⁴ the α -hydrogen of lactic acid being replaced by $-\text{CH}_2\text{COCO}_2^-$. It is interesting to note that the replacement of the α hydrogen of lactic acid by $-\text{CH}_2\text{COCO}_2^-$ has little effect on the acidity of the lactate carboxylate group. A similar effect is observed when a methyl hydrogen of acetic acid ($pK_a = 4.53$)¹⁴ is replaced by $-\text{CH}_2\text{COCO}_2^-$ to give α -ketoglutaric acid. There do not appear to be very significant inductive or electrostatic effects for $-\text{CH}_2\text{COCO}_2^-$.

(13) O. R. Buzzelli, Masters Thesis, The Ohio State University, 1966.

(14) L. G. Sillen and A. E. Martell, "Stability Constants of Metal Ion Complexes," 2nd ed, The Chemical Society, London, 1964.

The dimer dianion was found to form 1:1 and 2:1 complexes with both Ni(II) and Zn(II), and the stabilities of the complexes (Table I) are of the order observed with bidentate oxygen donors.¹⁴

The values of $\log K_{ex,D}$ are similar to those calculated for lactic acid¹⁴ (-1.9) rather than monohydrogen α -ketoglutarate (-3.3) or monohydrogen glutarate (-3.4). This suggests that chelate structure A predominates over B and C.



Pyruvate Dimerization Catalyzed by Nickel(II) and Zinc(II).

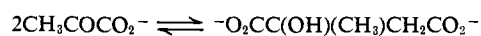
II. Kinetics¹

D. E. Tallman and D. L. Leussing

Contribution from the Department of Chemistry, Ohio State University, Columbus, Ohio 43210. Received April 7, 1969

Abstract: Ni(II) and Zn(II) catalyze pyruvate dimerization *via* a two-step reaction: enolate formation of complexed pyruvate followed by addition of a second pyruvate to the complexed enolate (carbanion). Proton loss from complexed pyruvate shows general base catalysis with water catalysis comprising the predominant path in the dilute acetate buffers employed. The rate of water-catalyzed proton removal is somewhat faster with Ni(II) than with Zn(II), but the reverse order of metal ion activity appears to hold for the addition reaction. This reactivity pattern can be ascribed to the differences in metal ion–enolate bond strengths with perhaps the ability of Zn(II) to form a less sterically constrained mixed complex contributing to a faster rate of addition. An approach is presented for correcting spectrophotometric rate data for time-dependent apparent deviations from Beer's law caused by changes in species distribution.

The catalytic effect of metal ions on pyruvate dimerization has been long known,² and metal ion ca-



talysis in other condensation-type reactions has also been reported^{3–6} but little quantitative information regarding the mode of metal ion activity appears to be available. Thus, a study of metal ion effects in pyruvate dimerization would provide pertinent information regarding an important class of reactions. Pyruvate dimerization can be conveniently followed spectrophotometrically because the intensity of absorption for the $315\text{-m}\mu \text{ n} \rightarrow \pi^*$ transition of the carbonyl group de-

creases by a factor of approximately 2 as two pyruvate ions (P^-) form one γ -methyl- σ -hydroxy- γ -ketoglutarate ion (D^{2-}). The recently completed study of the equilibrium properties of the Ni(II) and Zn(II) pyruvate monomer–dimer systems⁷ permits the evaluation of the extinction coefficients for the dimeric species, and therefore an analysis of spectrophotometric rate data becomes possible.

The calculation of rate constants for systems such as the present, which contain labile metal ions and reacting ligands in comparable concentrations, in general, is complicated by changes in the distribution of product and reactant species as the reaction proceeds. These concentration changes not only cause time-dependent variations in the rate law terms, but, if reactant or product species have different extinction coefficients, apparent time-dependent deviations from Beer's law are introduced into a rate function derived from spectrophotometric results. The availability of high-speed computers now makes it possible to easily correct for

(1) This project was supported by a grant from the National Science Foundation.

(2) L. Wolff, *Ann. Chem.*, **260**, 126 (1890); **305**, 154 (1899).

(3) M. L. Bender, "Reactions of Coordinated Ligands," *Advances in Chemistry Series*, No. 37, American Chemical Society, Washington D. C., 1963, Chapter 2.

(4) L. Benoiton, M. Winitz, R. F. Colman, M. Birnbaum, and J. P. Greenstein, *J. Am. Chem. Soc.*, **81**, 1726 (1959).

(5) P. N. Gordan, *J. Org. Chem.*, **22**, 1006 (1957).

(6) D. A. Fraser, R. W. Hall, and A. L. J. Raum, *J. Appl. Chem.*, **7**, 676 (1957); D. A. Fraser, R. W. Hall, P. A. Jenkins, and A. L. J. Raum, *ibid.*, **7**, 689 (1957).

(7) D. E. Tallman and D. L. Leussing, *J. Am. Chem. Soc.*, **91**, 6253 (1969).

such effects in many cases, and one approach to the solution of this problem is presented below.

Experimental Section

Stock solutions of sodium pyruvate, NiCl₂, and ZnCl₂ were prepared and standardized according to accepted methods. Reaction conditions were the same as those previously used,⁷ $\mu = 1.0$ (25°).

Extinction coefficients of the pyruvate species at 315 m μ have been determined in the investigation reported in ref 7. The extinction coefficients of D²⁻, HD⁻, H₂D, and MD (M²⁺ = Ni(II), Zn(II)) were calculated from the results of absorbance measurements on a series of solutions which were prepared so that each one of the solutions contained a particular form of the dimer as the predominant species. The equilibrium constants⁷ permitted the species distribution to be calculated for each solution, and the extinction coefficients reported in Table I were obtained by solving the resulting set of simultaneous equations.

Preliminary experiments showed that reaction rates were too slow for convenient study at the pH where pyruvate serves as a buffer, so dilute acetate buffering was employed. To keep complications arising from acetate complexing to a minimum, the total concentration of acetate was maintained at 0.020 M ([HAc] + [Ac⁻]).

A typical rate experiment was performed in the following way: a solution of sodium pyruvate containing acetate buffer was prepared immediately before use and placed in a constant-temperature water bath. The concentration of pyruvate in the solution was twice the concentration desired in the final reaction solution and the concentration of acetate buffer was 0.04 M. Sufficient NaCl was included in the solution to give an ionic strength of 1.0 M in the final reaction solution. A stock solution of the metal containing twice the concentration of metal desired in the final reaction solution was also allowed to come to thermal equilibrium in the constant-temperature bath. After thermal equilibration, equal volumes of the two solutions were mixed with vigorous stirring, and a portion was quickly placed in an absorbance cell. The cell was then placed into the thermostated cell holder of a Cary 14 spectrophotometer, and the absorbance was recorded as a function of time. Simultaneously the pH of the reaction solution remaining in the reaction vessel was recorded. In keeping with the basicity differences between monomer and dimer,⁷ the pH was found to increase as the reaction proceeded. Because of the presence of the acetate buffer, however, the change was very slow, seldom amounting to more than 0.001–0.002 pH unit/min. The pH of the solution was thus taken to be the value read from the pH meter within a period no longer than 4 min after metal addition. The small change in pH during this period has a negligible effect on the results.

The initial slope of the absorbance–time curve was determined by extrapolation to zero time. Owing to only a small curvature, the error in the initial slope is estimated to be less than 10% for most cases.

Blanks run in the absence of metal ion showed no detectable dimerization of pyruvate by the acetate buffer during the time of the experiments.

Analysis of the Data

At zero time, the reaction solution contains the complexes of pyruvate (MP⁺ and MP₂), protonated and unprotonated forms of pyruvate (HP and P⁻), and the metal ions and protons (M²⁺ and H⁺). The absorbance of the solution at this point is the sum of the absorbancies of these species. After zero time, the absorbance decreases due to the formation of dimer, and the solution then also contains the dimer complex, MD (MD₂ is negligible), as well as protonated and unprotonated dimer (H₂D, HD⁻, and D²⁻). The protonation and complex ion formation rates are rapid compared to the rate of dimer formation. Therefore, separate equilibria among the pyruvate species, on the one hand, and the dimer species, on the other hand, obtain. These two systems are not independent since each affects the other through its influence on the metal ion concentration (hydrogen ion activity being held constant.) The formation of metal ion–dimer complexes causes the value of [M²⁺] to decrease as the dimer concentration

builds up. This variation in [M²⁺] in turn causes the concentrations of uncomplexed forms to increase relative to complexed. Since the extinction coefficients of these various species differ (Table I), a perturbation is

Table I. Molar Extinction Coefficients (l. M⁻¹ cm⁻¹) of the Various Species of Monomeric and Dimeric Pyruvate (λ 315 m μ)

ϵ_P 22.1 ^a ϵ_{HP} 6.24 ^a	ϵ_D 23.1 ϵ_{HD} 16.5	ϵ_{H_2D} 8.6	
	ϵ_{MP}^a	$\epsilon_{MP_2}^a$	ϵ_{MD}
Ni(II)	25.8	66.1	30.8
Zn(II)	18.6	38.4	19.9

^aReference 7. P = pyruvate, D = γ -methyl- γ -hydroxy- α -keto-glutarate.

introduced into the rate of change of the absorbance. A correction must be made for this effect if correct rates are to be obtained.

In order to calculate the initial rates of formation of the dimer in the reaction solutions, it is necessary to know the solution composition at zero time. For each reaction solution, three mass balance equations can be set up

$$C_M = [M] + [MP] + [MP_2] + [MAc] + [MAc_2] \quad (1)$$

$$C_P = [P] + [MP] + 2[MP_2] + [HP] \quad (2)$$

$$C_{Ac} = [Ac] + [MAc] + 2[MAc_2] + [HAc] \quad (3)$$

where the terms on the left-hand side are known total concentrations and those on the right-hand side represent equilibrium concentrations. Invoking equilibrium these equations can be rewritten in terms of pyruvate (P⁻), acetate (Ac⁻), metal ion (M²⁺), and a_H .

$$C_M = [M^{2+}](1 + \beta_{1P}[P^-] + \beta_{2P}[P^-]^2 + \beta_{1Ac}[Ac^-] + \beta_{2Ac}[Ac^-]^2) \quad (4)$$

$$C_P = [P^-](1 + a_H/K_{a,P} + \beta_{1P}[M^{2+}] + 2\beta_{2P}[M^{2+}][P^-]) \quad (5)$$

$$C_{Ac} = [Ac^-](1 + a_H/K_{a,Ac} + \beta_{1Ac}[M^{2+}] + 2\beta_{2Ac}[M^{2+}][Ac^-]) \quad (6)$$

The acetate complexes are relatively minor components (<10% of total [M]) so it is satisfactory to use estimates from constants reported^{8,9} in the literature for similar conditions.¹⁰ The other necessary constants are given in ref 7. Since a_H is known from the measured pa_H , eq 4–6 may be solved for [M²⁺], [P⁻], and [Ac⁻].

The relationship between dimer formation and the absorbance change is obtained from similar mass balance expressions, which also include dimer terms, and an equation for the absorbance. For any point on the absorbance–time curve then

$$C_M = [M^{2+}] + [MP^+] + [MP_2] + [MAc^+] + [MAc_2] + [MD] \quad (7)$$

$$P_t = [P^-] + [HP] + [MP^+] + 2[MP_2] \quad (8)$$

(8) (a) L. G. Sillen and A. E. Martell, "Stability Constants of Metal Ion Complexes," 2nd ed, The Chemical Society, London, 1964; (b) P. Gerding, *Acta Chem. Scand.*, **21**, 2015 (1967).

(9) S. Kilpi and E. Lindel, *Suomen Kemistilehti*, **B36**, 81 (1963).

(10) $pK_{a,Ac} = 4.528$,⁹ $\log \beta_{1NiAc} = 1.0$, $\log \beta_{1Ni(Ac)_2} = 1.2$, $\log \beta_{2HAc} = 1.0$, $\log \beta_{Zn(Ac)_2} = 1.2$.

$$D_t = [D^{2-}] + [HD^-] + [H_2D] + [MD] \quad (9)$$

$$C_{P_{tot}} = [P_t] + 2[D_t] \quad (10)$$

$$C_{Ac} = [Ac^-] + [HAc] + [MAc^+] + 2[MAc_2] \quad (11)$$

$$A = (\epsilon_P[P^-] + \epsilon_D[D^{2-}] + \epsilon_{MP}[MP^+] + \epsilon_{MP_2}[MP_2] + \epsilon_{MD}[MD] + \epsilon_{HP}[HP] + \epsilon_{HD}[HD^-] + \epsilon_{H_2D}[H_2D])/l \quad (12)$$

where at time t , P_t is the total concentration of monomeric pyruvate, D_t is the total concentration dimeric pyruvate, P_t and D_t are related by eq 10 to the total initial concentration of pyruvate, $C_{P_{tot}}$, and l is the cell length. Expressing eq 7-12 in terms of all the constants pertaining to the system yields

$$C_M = [M^{2+}](1 + \beta_{1P}[P^-] + \beta_{2P}[P^-]^2 + \beta_{1Ac}[Ac^-] + \beta_{2Ac}[Ac^-]^2 + \beta_{1D}[D^{2-}]) \quad (13)$$

$$P_t = [P^-](1 + a_H/K_{a,P} + \beta_{1P}[M^{2+}] + 2\beta_{2P}[M^{2+}][P^-]) \quad (14)$$

$$D_t = [D^{2-}](1 + a_H/K_{a,2D} + a_H^2/K_{a,1D}/K_{a,2D} + \beta_{1D}[M^{2+}]) \quad (15)$$

$$C_{P_{tot}} = P_t + 2D_t \quad (16)$$

$$C_{Ac} = [Ac^-](1 + a_H/K_{a,Ac} + \beta_{1Ac}[M^{2+}] + 2\beta_{2Ac}[M^{2+}][Ac^-]) \quad (17)$$

$$A/l = \epsilon_P[P^-] + \epsilon_D[D^{2-}] + [M^{2+}](\epsilon_{MP}\beta_{1P}[P^-] + \epsilon_{MP_2}\beta_{2P}[P^-]^2 + \beta_{1D}\epsilon_{MD}[D^{2-}]) + a_H(\epsilon_{HP}[P^-]/K_{a,P} + \epsilon_{HD}[D^{2-}]/K_{a,D} + \epsilon_{H_2D}[D^{2-}]a_H/K_{a,1D}/K_{a,2D}) \quad (18)$$

Differentiating with respect to time at constant a_H and setting the concentrations of dimer species equal to zero at $t = 0$ gives

$$dC_M/dt = (1 + \beta_{1P}[P^-] + \beta_{2P}[P^-]^2 + \beta_{1Ac}[Ac^-] + \beta_{2Ac}[Ac^-]^2) d[M^{2+}]/dt + [M^{2+}](\beta_{1P} + 2\beta_{2P}[P^-]) d[P^-]/dt + [M^{2+}](\beta_{1Ac} + 2\beta_{2Ac}[Ac^-]) d[Ac^-]/dt + [M^{2+}]\beta_{1D} d[D^{2-}]/dt \quad (19)$$

$$dP_t/dt = (1 + a_H/K_{a,P} + \beta_{1P}[M^{2+}] + 4\beta_{2P}[M^{2+}][P^-]) d[P^-]/dt + [P^-](\beta_{1P} + 2\beta_{2P}[P^-]) d[M^{2+}]/dt \quad (20)$$

$$dD_t/dt = (1 + a_H/K_{a,2D} + a_H^2/K_{a,1D}/K_{a,2D} + \beta_{1D}[M^{2+}]) d[D^{2-}]/dt \quad (21)$$

$$dC_P/dt = dP_t/dt + 2dD_t/dt \quad (22)$$

$$dC_{Ac}/dt = (1 + a_H/K_{a,Ac} + \beta_{1Ac}[M^{2+}] + 4\beta_{2Ac}[M^{2+}][Ac^-]) d[Ac^-]/dt + [Ac^-](\beta_{1Ac} + 2\beta_{2Ac}[Ac^-]) d[M^{2+}]/dt \quad (23)$$

$$(dA/dt)/l = (\epsilon_P + \epsilon_{MP}\beta_{1P}[M^{2+}] + 2\epsilon_{MP_2}\beta_{2P}[M^{2+}][P^-] + a_H\epsilon_{HP}/K_{a,P}) d[P^-]/dt + (\epsilon_D + \epsilon_{MD}\beta_{1D}[M^{2+}] + a_H\epsilon_{HD}/K_{a,2D} + a_H^2\epsilon_{H_2D}/K_{a,1D}/K_{a,2D}) d[D^{2-}]/dt + (\epsilon_{MP}\beta_{1P}[P^-] + \epsilon_{MP_2}\beta_{2P}[P^-]^2) d[M^{2+}]/dt \quad (24)$$

The quantities dC_P/dt , dC_{Ac}/dt , and dC_M/dt are the rates of change of the total concentrations of pyruvate (monomer plus dimer), acetate, and metal, respectively,

and are equal to zero since the volume of the solution remains constant throughout the run. The value of dA/dt , the rate of change of the absorbance of the reaction solution, is obtained from the slope of the absorbance-time curve. The values of all the constants are known and the concentrations of the species (M^{2+} , P^- , and Ac^-) are first calculated from eq 4-6; a_H is known from the measured pH. Therefore, eq 19-24 are linear in the six unknowns, $d[M^{2+}]/dt$, $d[P^-]/dt$, $d[D^{2-}]/dt$, $d[Ac^-]/dt$, dP_t/dt , and dD_t/dt , and can be solved for these quantities. The unknown variables $d[M^{2+}]/dt$, $d[P^-]/dt$, $d[D^{2-}]/dt$, and $d[Ac^-]/dt$ are the time rates of change of the free (unprotonated and uncomplexed) concentrations of metal, pyruvate, dimer, and acetate, respectively. The quantities dP_t/dt and dD_t/dt are the rate of total monomeric pyruvate disappearance and the desired rate of total dimeric pyruvate formation. The calculated solution compositions and values of dD_t/dt obtained for the Ni(II) and Zn(II) systems in the present investigation are given in Tables II and III.

Table II. Rates of the Ni(II)-Promoted Dimerization of Pyruvate

Expt no.	$[Ni^{2+}]_{free} \times 10^2, M$	$[P^-]_{free} \times 10^2, M$	$[Ac^-]_{free} \times 10^3, M$	pH	$dD_t/dt \times 10^6, M \text{ sec}^{-1}$
1	9.78	2.73	5.55	4.322	2.87
2	8.13	5.76	6.06	4.360	6.69
3	6.81	9.03	6.48	4.385	10.60
4	15.32	2.20	4.52	4.255	3.76
5	13.10	4.66	4.92	4.288	8.18
6	11.21	7.37	5.33	4.320	12.45
7	21.06	1.84	3.80	4.200	4.72
8	18.41	3.88	4.12	4.230	9.70
9	16.07	6.15	4.48	4.265	13.52
10	4.59	3.56	7.12	4.400	1.65
11	3.68	7.39	7.60	4.430	3.97
12	3.00	11.42	8.07	4.460	6.51
13	9.61	2.78	7.43	4.677	3.56
14	7.98	5.85	8.05	4.705	8.40
15	6.68	9.16	8.57	4.717	11.42
16	15.12	2.23	5.92	4.606	4.46
17	12.92	4.71	6.43	4.628	9.42
18	11.07	7.43	6.88	4.638	14.25
19	20.84	1.85	4.90	4.544	5.74
20	18.21	3.91	5.31	4.566	10.45
21	15.90	6.19	5.72	4.585	17.43
22	4.49	3.60	9.70	4.750	2.36
23	3.61	7.46	10.3	4.770	5.10
24	2.95	11.52	10.8	4.794	9.20
25	9.99	2.70	3.19	3.898	1.78
26	8.29	5.70	3.67	3.970	4.09
27	6.92	8.97	4.06	4.020	6.74
28	15.59	2.17	2.65	3.830	2.31
29	13.32	4.61	2.99	3.890	5.72
30	11.40	7.29	3.34	3.945	9.09
31	21.38	1.81	2.24	3.765	2.70
32	18.68	3.84	2.56	3.835	6.62
33	16.31	6.08	2.86	3.890	10.17
34	4.72	3.51	3.87	3.960	1.06
35	3.77	7.30	4.41	4.930	2.62
36	3.07	11.30	4.90	4.085	4.44

Results and Discussion

The α -carbonyl group in pyruvic acid is considerably more hydrated (45%) than it is in the pyruvate ion (3%).¹¹⁻¹⁴ This difference essentially accounts for the

(11) M. Becker and H. Strehlow, *Z. Elektrochem.*, **64**, 813 (1960).

(12) M. Becker, *Ber. Bunsenges. Physik. Chem.*, **68**, 669 (1964).

(13) D. L. Leussing and C. K. Stanfield, *J. Am. Chem. Soc.*, **86**, 2805 (1964).

Table III. Rates of the Zn(II)-Promoted Dimerization of Pyruvate

Expt no.	[Zn ²⁺] _{free} × 10 ³ , M	[P ⁻] _{free} × 10 ³ , M	[Ac ⁻] _{free} × 10 ³ , M	p _{aH}	dD _t /dt × 10 ⁶ , M sec ⁻¹
1	9.34	1.85	4.20	4.080	1.63
2	7.15	3.86	4.71	4.128	3.86
3	5.43	6.11	5.17	4.165	6.19
4	13.78	1.46	4.30	4.175	1.98
5	11.17	3.00	4.75	4.210	4.14
6	8.99	4.71	5.23	4.247	7.74
7	20.81	1.10	3.40	4.083	1.77
8	17.73	2.26	3.74	4.120	4.37
9	15.03	3.50	4.07	4.150	7.22
10	9.12	1.86	7.22	4.605	1.78
11	7.02	3.86	7.98	4.632	4.63
12	5.36	6.10	8.67	4.650	6.86
13	11.01	3.03	6.53	4.555	5.39
14	17.53	2.28	5.04	4.452	5.90
15	14.85	3.53	5.51	4.480	9.14
16	14.04	1.43	2.42	3.760	0.71
17	11.40	2.95	2.76	3.820	2.90
18	9.17	4.63	3.11	3.875	5.49
19	2.83	5.69	7.46	4.385	2.31
20	1.96	9.01	7.96	4.410	4.20
21	4.00	2.74	9.62	4.704	1.33
22	2.77	5.73	10.4	4.724	2.91
23	1.93	9.07	11.0	4.740	4.34
24	9.13	1.85	7.20	4.602	1.83
25	8.87	4.73	7.13	4.575	8.03
26	20.58	1.11	4.62	4.435	2.54
27	21.11	1.09	1.94	3.670	0.74
28	15.25	3.47	2.48	3.785	5.45
29	7.31	3.76	3.29	3.890	2.79
30	5.58	5.95	3.71	3.945	4.80

considerably lower extinction coefficient of pyruvic acid at 315 μ . The successive decrease observed in Table I on increasing the protonation of the dimer most likely arises from the same reason. A similar relationship is observed between the extinction coefficients of D²⁻ and H₂D as is observed between those for P⁻ and HP. The somewhat low value of ϵ_{HD} compared to ϵ_a no doubt indicates some protonation of the keto carboxylate group of HD⁻ although the methylene carboxylate is more basic.

Rates

Initial calculations of the kinetic data indicated that, within experimental error, the rate of formation of pyruvate dimer is first order with respect to metal ion. The dependence of the rate upon the pyruvate and hydrogen ion concentrations, however, was found not to be so simple. The rate is between first and second order in pyruvate and between zero and first order in the reciprocal of hydrogen ion concentration conforming to the rate law

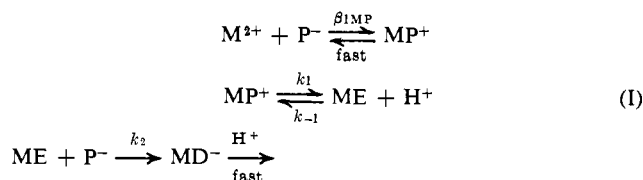
$$\frac{dD_t}{dt} = \frac{k_1'[M^{2+}][P^-]^2}{k_2'[H^+] + [P^-]} \quad (25)$$

The inverse dependence on H⁺ suggests rate-determining enolate formation but the value of k_1' ($k_1' \sim k_1''$ of Table V) was found to be considerably greater than expected considering the reported pseudo-first-order constant of 9.4×10^{-8} sec⁻¹ for water-catalyzed enolization of pyruvate.¹⁵ This observation and the form of

(14) V. S. Griffiths and G. Socrates, *Trans. Faraday Soc.*, **63**, 673 (1967).

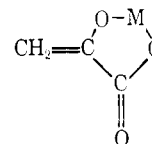
(15) W. J. Albery, R. P. Bell, and A. L. Powell, *ibid.*, **61**, 1194 (1965).

the rate law indicates that metal ion is involved in the enolization according to the reaction scheme



equilibrium distribution of H₂D, HD⁻, D²⁻, and MD

Here ME represents the complexed deprotonated enolate of pyruvate ion



The enolate complex, ME, is present in low concentration and application of the steady-state approximation yields

$$k_1' = k_1\beta_{1MP} \text{ and } k_2' = k_{-1}/k_2$$

Calculations were made assuming that addition also proceeds *via* a path involving dissociated enolate: $ME \rightleftharpoons M^{2+} + E^{2-}$; $E^{2-} + P^- \rightarrow$ dimer. This path introduces M^{2+} in the denominator of (25), and no such dependence was indicated.

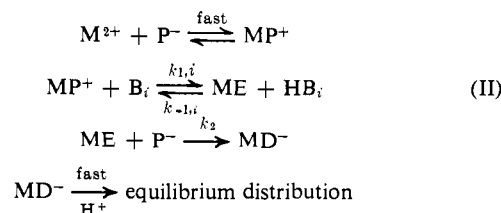
Reaction scheme I accounts for the principal features of the rate behavior, but trends in the data indicated acetate and, possibly, pyruvate catalysis. Acetate catalysis is demonstrated in a series of experiments, the results of which are shown in Table IV, where Ni(II),

Table IV. Rate of Dimerization as a Function of Acetate Concentration

C_{Ni} , M	C_P , M	pH	[Ac ⁻], M × 10 ³	Rate, M sec ⁻¹ × 10 ⁶
0.1866	0.04935	4.250	4.49	3.60
0.1866	0.04935	4.245	9.03	4.16
0.1866	0.04935	4.248	13.7	4.96

pyruvate, and hydrogen ion activity were held constant while the buffer concentration was varied at a constant ratio of HAc to Ac⁻. The rate is seen to increase as the buffer concentration increases, indicating that acetate and/or acetic acid catalysis occurs. The data of Tables II and III are compatible with acetate and not with acetic acid catalysis, however.

Rate expression 25 was then modified to take into account general base catalysis.



The rate equation becomes

$$\frac{dD_t}{dt} = \frac{[M^{2+}][P^-]^2(k_1'' + k_2''[-OAc] + k_3''[P^-])}{(k_4'' + k_5''[-OAc] + k_6''[P^-])[H^+] + [P^-]} \quad (26)$$

Table V. Values of the Rate Constants (25°, $\mu = 1.0$)

	$k_1'', M^{-1} \text{sec}^{-1}$	$k_2'', M^{-2} \text{sec}^{-1}$	Constants for Eq 26		k_5'', M^{-1}	k_6'', M^{-1}
			$k_3'', M^{-2} \text{sec}^{-1}$	$k_4''^a$		
Ni(II)	$2.4 \pm 0.3 \times 10^{-3}$	$(6.5 \times 10^{-3})^b$	(4×10^{-4})	(0-180)	$1.27 \pm 0.5 \times 10^3$	$(7.8) \times 10^3$
Zn(II)	$1.67 \pm 0.28 \times 10^{-3}$	(3.8×10^{-3})	(2.4×10^{-3})	220 ± 110	$(9.1) \times 10^3$	$(5.6) \times 10^3$

	Constants for the Generalized Rate Law II					
	$k_{1H_2O}, \text{sec}^{-1}$	$k_{1Ac}, M^{-1} \text{sec}^{-1}$	$k_{1P}, M^{-1} \text{sec}^{-1}$	$k_{-1H_2O^+}/k_2$	k_{-1HAc}/k_2	k_{-1HP}/k_2
Ni(II)	$3.2 \pm 0.4 \times 10^{-4}$	(9×10^{-4})	(5×10^{-5})	(0-180)	3.7	62
Zn(II)	$1.15 \pm 0.19 \times 10^{-4}$	(2.6×10^{-3})	(1.6×10^{-4})	220 ± 110	(0.27)	(4.5)

^a In computing these values a_H was converted to concentration units using the empirically determined relationship for the glass electrode system in the media: $\text{pH} = 1.014\text{p}a_H + 0.042$. ^b Values enclosed in parentheses have an uncertainty of a factor of 2 or more.

Pyruvate catalysis is not sufficiently important relative to the precision of the data to warrant an independent evaluation of k_3'' and k_6'' . Because of this the Brønsted catalysis law, $k_p/k_{ac} = (K_{a,Ac}/K_{a,P})^\beta$, was invoked to relate the pyruvate rate constants to those of acetate. The value of β for base-catalyzed halogenation reactions of carbonyl compounds for which the rate of C-H cleavage is of the order observed in the present study lie in the range 0.4-0.6^{16,17} so an intermediate value of 0.5

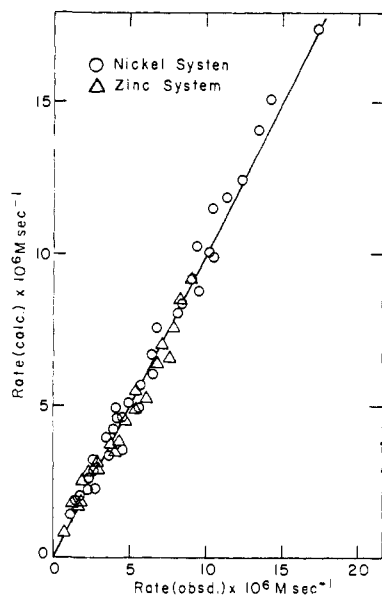


Figure 1. A comparison of observed and calculated rates (eq 26).

was taken. The choice of β is not critical since the calculations revealed that the pyruvate path contributes less than 10% to the observed rate. With β equal to 0.5, $k_3'' = 0.0614k_2''$ and $k_6'' = 0.0614k_5''$. Using these relationships the values of the parameters k_1'' , k_2'' , k_4'' , and k_5'' which give the best fit of eq 26 to the data were found using a "pit-map" procedure⁷ in which the minimum sum square for differences between observed and calculated rates was located. The rate constants are presented in Table V. The comparison of the observed rates with those calculated using the values in Table V is obtained by inspection of Figure 1.

The values found for k_1'' under the conditions investigated have the least uncertainty since water-catalyzed proton loss from complexed pyruvate (enolate forma-

tion) is somewhat more important than the subsequent pyruvate addition step or the relatively slight catalysis by the dilute acetate or weakly basic pyruvate ions. The results for these last steps have appreciable uncertainty and are best considered as rough values. Applying the steady-state approximation to the intermediate metal-enolate complex yields the relationships: $k_{1H_2O} = k_1''/\beta_{MP}$, $k_{1Ac} = k_2''/\beta_{MP}$, $k_{1P} = k_3''/\beta_{MP}$, $k_{-1H_2O^+}/k_2 = k_4''$, $k_{-1HAc}/k_2 = k_5''K_{a,Ac}$, $k_{-1HP}/k_2 = k_6''K_{a,P}$. Values of these rate constants and rate constant ratios are also presented in Table V.

Values of k_{1H_2O} found here for complexed pyruvate are of the order of 250-1000 times greater than those reported¹⁵ for enolization of pyruvic acid ($4.4 \times 10^{-7} \text{sec}^{-1}$) and uncomplexed pyruvate ($9.4 \times 10^{-8} \text{sec}^{-1}$). The term for acetate catalysis is also enhanced by complexation but perhaps by a smaller factor. Schellenberger and Hubner¹⁸ report a value of $5 \times 10^{-6} M^{-1} \text{sec}^{-1}$ for the acetate-catalyzed enolization as obtained from the rate of pyruvate halogenation. Furthermore, halogenation rates¹⁹ show similar metal ion effects as found here for dimerization. The agreement supports the postulate of enolization as the primary rate-determining step in these processes. The high activity of the metal ion compared to even the proton no doubt lies in its ability to stabilize the enolate through chelate ring formation. Additional evidence for this lies in the fact that the k_{1H_2O} terms vary with the metal ions in the same direction as do those quantities which are a measure of metal ion-oxygen bond strengths, *i.e.*, electronegativities, hydration energies, or stabilities of the oxalate complexes. This point was qualitatively tested further by comparing the reactivity of Cd(II) with Ni(II) and Zn(II) under similar conditions. The results are presented in Table VI where it is observed that the order of reactivities, which is determined principally by enolization rates, follows the electronegativities: Ni(II) > Zn(II) >> Cd(II). The pH difference between the Ni(II) run and those of the other two metal ions in Table VI ac-

Table VI. Comparison of the Relative Dimerization Rates with Different Metal Ions

M	C_M	C_P	C_{Ac}	pH	Rel rate	Electronegativity ^a
Ni(II)	0.124	0.098	0.020	4.36	21	5.3
Zn(II)	0.125	0.100	0.020	4.13	11	4.9
Cd(II)	0.125	0.100	0.020	4.13	1	3.9

^a A. L. Allred and E. G. Rochow, *J. Inorg. Nucl. Chem.*, **5**, 264 (1958).

(18) A. Schellenberger and G. Hubner, *Chem. Ber.*, **98**, 1938 (1965).

(19) A. Schellenberger, R. Lorenz, G. Oehme, and H. Diescher, *J. Prakt. Chem.*, **24**, 239 (1964).

(16) R. P. Bell, "The Proton in Chemistry," Cornell University Press, Ithaca, N. Y., 1959.

(17) E. Kosower, "Physical Organic Chemistry," John Wiley and Sons, Inc., New York, N. Y., 1968.

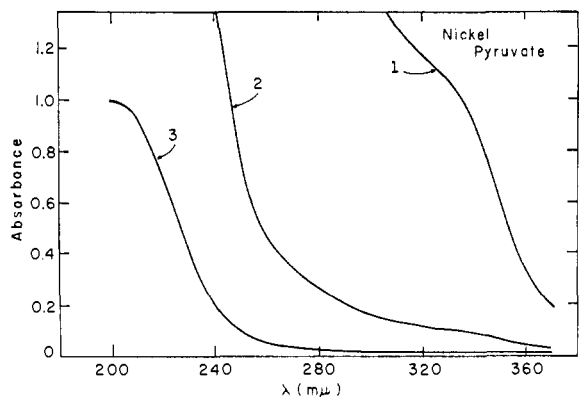


Figure 2. Uv absorption spectrum of NiP^+ : 0.249 M NiCl_2 , 0.050 M NaP , 0.020 M acetate buffer (pH 4.54, $\mu = 1.0$). Cell lengths (cm) for curves are as follows: (1) 1.00, (2) 0.100, (3) 0.010. Reference blank identical except for NaP which was omitted. The spectrum was completed within 4 min after solution preparation.

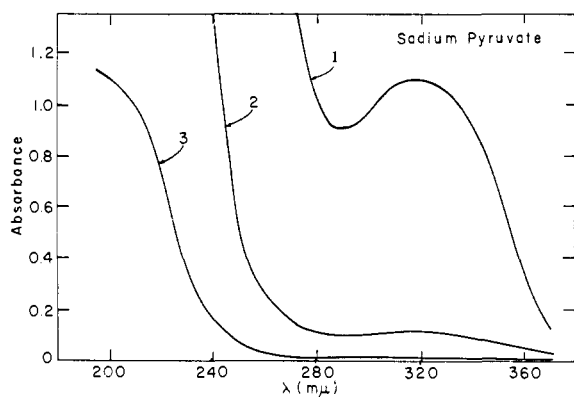


Figure 3. Uv absorption spectrum of NaP : 0.050 M NaP , 0.020 M acetate/buffer (pH 5.15, $\mu = 1.0$); see also legend for Figure 2.

counts for only a small part of the observed rate differences.

The absorption spectra of pyruvate complexes involving divalent first-row transition metal ions do not show readily distinguishable features which are attributable to enolate forms.^{20,21} However, spectral changes which occur during the decarboxylation of oxaloacetate complexes indicate that pyruvate enolate complexes have an absorption maximum somewhat below 295 $m\mu$ with extinction coefficients of several thousand.^{20,21} Enolate complexes of oxaloacetate exhibit a maximum at 295 with an extinction coefficient of 2×10^4 .^{20,21}

Spectral differences between nickel(II) pyruvate on one hand (Figure 2) and sodium and zinc(II) pyruvate on the other hand (Figures 3 and 4) suggests that a low but detectable concentration of enolate is present with Ni(II) . The Ni(II) spectrum of Figure 2 shows definite evidence for an absorbance maximum in the region of 285 $m\mu$. Subtracting the NaP absorbance at 285 $m\mu$ from that for Ni(II) and assuming an extinction coefficient of 10^4 yields an enolate content of about 0.2% for NiP^+ under the conditions employed.

The steady-state concentration of NiE is given by eq 26. Using the concentrations calculated for expt 19 of Table II, the rate constants given in Table I V, and a

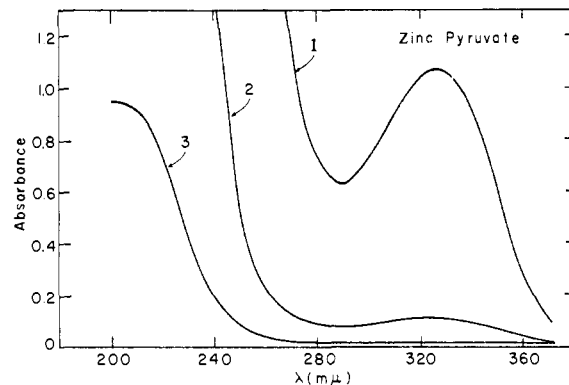
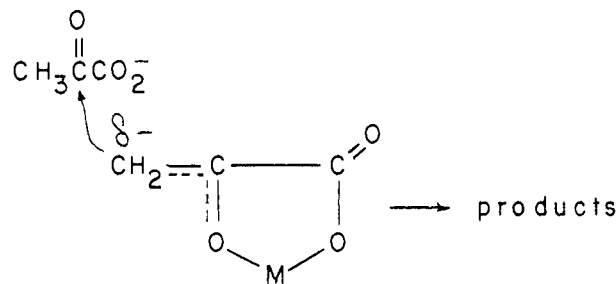


Figure 4. Uv absorption spectrum of ZnP^+ : 0.250 M ZnCl_2 , 0.050 M NaP , 0.020 M acetate buffer (pH 4.43, $\mu = 1.0$); see also legend for Figure 2.

$$[\text{NiE}] = \frac{[\text{Ni}^{2+}][\text{P}^-](k_{1\text{H}_2\text{O}} + k_{1\text{Ac}}[\text{Ac}^-] + k_{1\text{P}}[\text{P}^-])\beta_{\text{NiP}}}{\left(k_{-1\text{H}_2\text{O}} + \frac{k_{-1\text{HAc}}[\text{Ac}^-]}{K_{\text{a,Ac}}} + \frac{k_{-1\text{HP}}[\text{P}^-]}{K_{\text{aP}}}\right)[\text{H}^+] + k_2[\text{P}^-]} \quad (26)$$

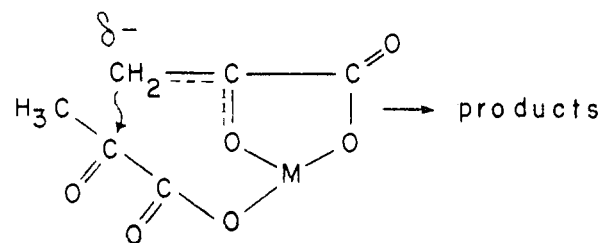
steady-state concentration of NiE of 0.2%, it is calculated that $k_2 \sim 1-10 \text{ M}^{-1} \text{ sec}^{-1}$. The low absorbance at 285 $m\mu$ for the zinc pyruvate solution together with the dimerization rate indicates that the Zn(II) enolate must be more reactive than the Ni(II) enolate both toward protons and pyruvate ions.

This reactivity pattern can be accounted for by either a second-order outer-sphere attack by pyruvate of complexed enolate



outer sphere

or a first-order inner-sphere mechanism



inner sphere

(promnastic)

Either path is expected to show the same type of dependence on the metal ion electronegativity since this factor will influence the carbanion-enolate ratio. A high

(20) E. Gelles and R. W. Hay, *J. Chem. Soc.*, 3673 (1958).

(21) E. Gelles and H. Salama, *ibid.*, 3683, 3689 (1958).

electronegativity should decrease k_2 by stabilizing the enolate form relative to the carbanion, thus decreasing the availability of the reactive species.

By virtue of a reduction from a second-order reaction to first order, the inner-sphere path presents an entropy advantage over the outer-sphere path. An inner-sphere path is plausible because complexing of pyruvate to the enolate complex, giving the mixed complex, $M(E)(P)$, is rapid, and molecular models show that in the mixed complex the carbonyl carbon of monodentately bound pyruvate can be brought almost into contact with the methylene group of the carbanion. For such an arrangement of ligands to be possible, the metal ion must not impose stringent steric requirements on the complexed pyruvate (the promnastic effect).²² In this re-

spect, an inner-sphere reaction possesses features in common with Schiff base formation where Zn(II) shows kinetic activity but Ni(II) is kinetically inactive.²² Qualitatively, the same order is indicated for k_2 in pyruvate dimerization. The reactivity of Ni(II) in the present system would be a consequence of its relatively small tendency to bind pyruvate compared to the glycinate of the previous work.²²

Because electronegativity and the promnastic effect should both cause k_2 for Zn(II) to be higher than that for Ni(II), the present qualitative data do not distinguish between the two possibilities. The entropy gain, however, would make the inner-sphere reaction more likely, other factors being constant.

(22) D. Hopgood and D. L. Leussing, *J. Am. Chem. Soc.*, **91**, 3740 (1969).

Unusual Metalloporphyrins. IV. Novel Methods for Metal Insertion into Porphyrins^{1a,b}

M. Tsutsui, R. A. Velapoldi, K. Suzuki, F. Vohwinkel, M. Ichikawa, and T. Koyano

Contribution from the Department of Chemistry, Texas A & M University, College Station, Texas 77843. Received May 16, 1969

Abstract: Several metalloporphyrins including the new chromium and titanium porphyrins have been synthesized by two novel metal insertion methods which use metal carbonyls and the σ -bonded organo-transition metal compound, diphenyltitanium. The compounds were characterized by infrared, ultraviolet, and visible spectra, magnetic susceptibilities, and elemental analyses. The chromium ion is in the dipositive oxidation state and the titanium ion is in the tetrapositive oxidation state as the titanyl species. Evidence for molecular aggregation of the chromium and titanyl porphyrins in the solid and in solution is presented. The applicability of the preparative methods and loss of carbonyl ligands are discussed.

Although metalloporphyrins are widely dispersed in nature²⁻⁴ and many have been synthesized, only those of chromium and titanium of the first-row transition metals have not been prepared,⁵ nor have they been identified in nature. It is proposed, however, that titanium porphyrins are present in crude petroleum.^{2,6} Vanadium porphyrins have been found in crude petroleum and have been synthesized under relatively severe conditions.^{2,3,7}

A series of metalloporphyrins including the chromium and vanadyl mesoporphyrins has been prepared by the facile metal insertion reaction using metal carbonyls. This method, however, was not applicable for the preparation of a titanium porphyrin since titanium carbonyls are unknown and attempts to prepare them are unsuccessful.⁸ Instead, a novel method of metal insertion into the porphyrin was developed using the σ -bonded organo-transition metal compound, diphenyltitanium. This paper presents these novel preparative methods and the characterizations of the prepared metalloporphyrins.

Experimental Section

Reagents, Solvents, and Instrumentation. Solvents used in the metalloporphyrin preparations by metal carbonyls were distilled under purified ^{9a} nitrogen while the solvents used in the titanium porphyrin preparation were distilled under purified argon from typical drying agents:^{9b} mesitylene, *n*-pentane, and *n*-hexane from sodium; benzene, toluene, and ether from lithium aluminum hydride. Decane and decalin were shaken with sulfuric acid,

(1) (a) Supported by National Science Foundation Grant GB-5732. (b) This work was reported in part in the preliminary communication: M. Tsutsui, M. Ichikawa, F. Vohwinkel, and K. Suzuki, *J. Amer. Chem. Soc.*, **88**, 854 (1966); M. Tsutsui, R. A. Velapoldi, K. Suzuki, and T. Koyano, *Angew. Chem.*, **7**, 891 (1968).

(2) A. Treibs, *Ann.*, **510**, 42 (1934); **517**, 172 (1935); B. J. Duffy and H. M. Hart, *Chem. Eng. Progr.*, **48**, 344 (1953); H. N. Dunning, J. W. Moore, and M. O. Denekas, *Ind. Eng. Chem.*, **45**, 1759 (1953); C. G. Dodd and J. W. Moss, *ibid.*, **44**, 2585 (1952); H. N. Dunning and N. A. Rabon, *ibid.*, **48**, 951 (1956); S. Groennings, *Anal. Chem.*, **25**, 938 (1953); J. Sanik, *Anal. Chim. Acta*, **21**, 572 (1959); A. A. Wolsky and F. W. Chapinan, Jr., *Proc. Am. Petrol. Inst., Sect. III*, **40**, 423 (1960).

(3) J. E. Falk, "Porphyrins and Metalloporphyrins," Elsevier Publishing Co., New York, N. Y., 1964.

(4) J. F. Taylor, *J. Biol. Chem.*, **135**, 569 (1940).

(5) The phthalocyanines of chromium and titanium have been prepared: (a) F. H. Moser and A. L. Thomas, "Phthalocyanine Compounds," Reinhold Publishing Co., New York, N. Y., 1963; (b) J. A. Elvidge and A. B. P. Lever, *J. Chem. Soc.*, 1257 (1961); A. B. P. Lever, Ph.D. Thesis, London, 1961.

(6) T. Muniyappan, *J. Chem. Educ.*, **32**, 277 (1955).

(7) J. G. Erdman, V. G. Ramsey, N. W. Kalenda, and W. E. Hanson, *J. Amer. Chem. Soc.*, **78**, 5844 (1956).

(8) M. Tsutsui, unpublished results.

(9) (a) Purified indicates bubbled through a Na-K alloy; (b) L. F. Fieser and M. Fieser, "Reagents for Organic Syntheses," John Wiley & Sons, Inc., New York, N. Y., 1967; L. F. Fieser, "Experiments in Organic Chemistry," D. C. Heath and Co., Boston, Mass., 1957.